Super-resolution of VIIRS-Measured Ocean Color Products Using Deep Convolutional Neural Network

Xiaoming Liu[1,2] and **Menghua Wang**[1]
[1]NOAA/NESDIS/STAR, Ocean Color Science Team
[2]Colorado State University, CIRA

The 2nd NOAA Workshop on AI, 11/12/2020

Website for VIIRS ocean color images, data and Cal/Val:
http://www.star.nesdis.noaa.gov/sod/mecb/color/

Outline

- Motivation
- Part I: Super-resolving VIIRS normalized water-leaving radiance spectra $nL_w(\lambda)$
  - Convolution Neural Networks
  - Training
  - Evaluation
  - Applications
- Part II: Super-resolving $nL_w(\lambda)$-derived products: $K_d(490)$ and Chl-a
  - Re-training networks
  - Evaluation
  - Applications
- Summary and Path Forward

Motivation

- Ocean color products derived from the Visible Infrared Imaging Radiometer Suite (VIIRS) on the Suomi National Polar-orbiting Partnership (SNPP) include normalized water-leaving radiance spectra $nL_w(\lambda)$ of five M-bands at the wavelengths of 410, 443, 486, 551 and 671 nm, and one I-band at 638 nm, $nL_w(638)$.
- Biological and biogeochemical products, such as chlorophyll-a (Chl-a) concentration and water diffuse attenuation coefficient at the wavelength of 490 nm ($K_d(490)$), are derived from $nL_w(\lambda)$ spectra.
- Spatial resolutions of VIIRS I-bands and M-bands are differed by a factor of two
  - M-band $nL_w(\lambda)$, $K_d(490)$ and Chl-a : 750 m
  - I-band $nL_w(638)$: 375 m
- It is useful to have high-spatial resolution data for M-band $nL_w(\lambda)$, $K_d(490)$ and Chl-a data with also 375 m, particularly over coastal/inland waters.
- Deep Convolutional Neural Network (CNN) is used to super-resolve $nL_w(\lambda)$, $K_d(490)$, and Chl-a at the M-bands from 750-m to 375-m spatial resolution.

Part I: Super-resolving VIIRS normalized water-leaving radiance spectra $nL_w(\lambda)$

Liu, X. and **M. Wang**, "Super-Resolution of VIIRS-Measured Ocean Color Products Using Deep Convolutional Neural Network", *IEEE Trans. Geosci. Remote Sens.* https://doi.org/10.1109/TGRS.2020.2992912 (2020).

$nL_w(\lambda)$ at VIIRS I-band and M-bands Images

Baltic Sea (14 August 2015)

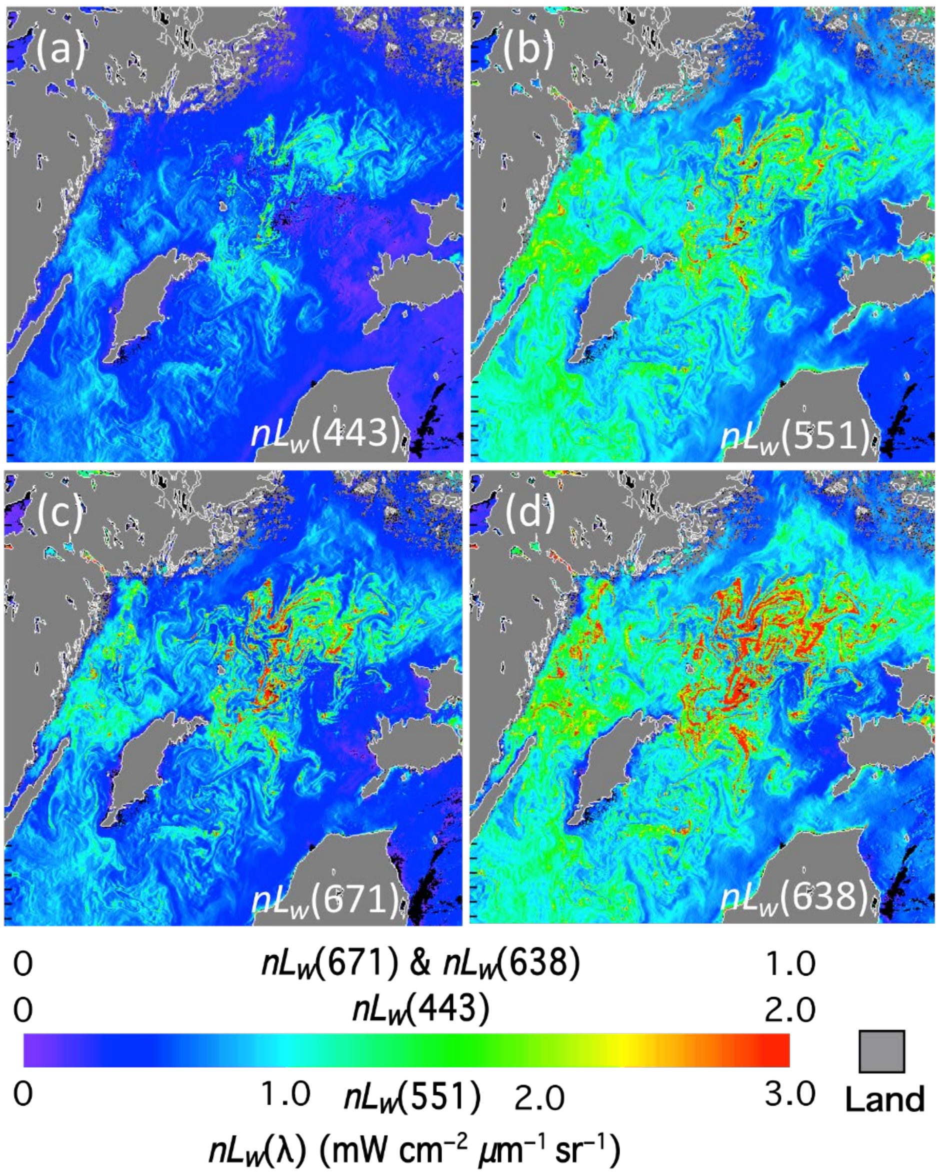

Bohai Sea (15 April 2019)

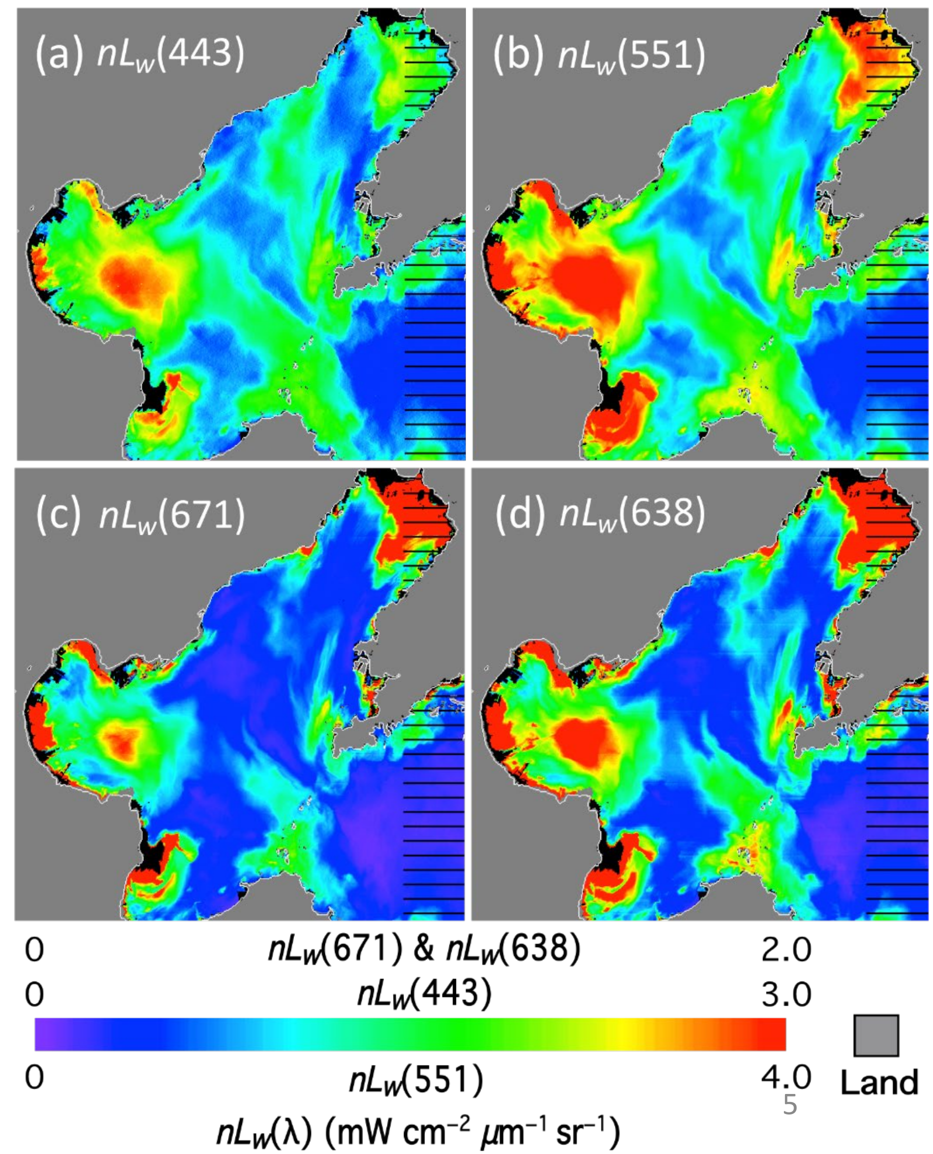

Correlation between I-band and M-bands

Correlation coefficient of $nL_w(\lambda)$ between at the M-bands and the I1 band, $nL_w(638)$, in the Baltic Sea and Bohai Sea.

Parameter	Baltic Sea	Bohai Sea
$nL_w(410)$	0.8572	0.8181
$nL_w(443)$	0.8691	0.8550
$nL_w(486)$	0.8977	0.8601
$nL_w(551)$	0.9397	0.9077
$nL_w(671)$	0.9946	0.9942
$nL_w(745)$	0.6658	0.8229

Convolutional Neural Networks

- CNN developed by Lanaras et al. (2018)

  C. Lanaras, J. Bioucas-Dias, S. Galliani, E. Baltsavias, and K. Schindler, “Super-resolution of Sentinel-2 images: Learning a globally applicable deep neural network,” ISPRS J. Photogramm. Remote Sens. , vol. 146, pp. 305–319, doi:10.1016/j.isprsjprs.2018.09.018, 2018.

- One network for each M-band in two regions
  - Baltic Sea: CNN-Baltic-$nL_w(\lambda)$
  - Bohai Sea: CNN-Bohai-$nL_w(\lambda)$
- Assumption: networks trained for super-resolving images on a lower scale from 1.5-km to 750-m spatial resolution are also valid for super-resolving $nL_w(\lambda)$ images on the original scale from 750-m to 375-m spatial resolution (Shechtman et al. 2007, Glasner et al. 2009)
- The networks are implemented with TensorFlow (version 1.2.1) in Python (version 3.6.7) environment, and trained on CentOS 6.10 with four core Intel(R) Xeon(R) CPU E7-4820 of 2.00 GHz and 128 GB memory.

Training Data

List of VIIRS granules and data acquired dates for training networks in the **Baltic Sea** and **Bohai Sea**.

	CNN-Baltic-$nL_w(\lambda)$		CNN-Bohai-$nL_w(\lambda)$	
	Granule	Date	Granule	Date
1	V2019070042852	03/11/2019	V2015213113614	08/01/2015
2	V2019073051140	03/14/2019	V2015215105822	08/03/2015
3	V2019073051305	03/14/2019	V2015216103927	08/04/2015
4	V2019074045411	03/15/2019	V2015221104550	08/09/2015
5	V2019075043516	03/16/2019	V2015223114859	08/11/2015
6	V2019084050531	03/25/2019	V2015225111108	08/13/2015
7	V2019090045259	03/31/2019	V2015227103444	08/15/2015
8	V2019091043404	04/01/2019	V2015228115523	08/16/2015
9	V2019100050545	04/10/2019	V2015229113502	08/17/2015
10	V2019106045313	04/16/2019	V2015229113627	08/17/2015
11	V2019116050558	04/26/2019	V2015230111606	08/18/2015
12	V2019121051222	05/01/2019	V2015230111731	08/18/2015
13	V2019126051846	05/06/2019	V2015231105836	08/19/2015
14	V2019127045950	05/07/2019	V2015232103942	08/20/2015
15	V2019143050004	05/23/2019	V2015235112355	08/23/2015

https://www.star.nesdis.noaa.gov/sod/mecb/color/

Evaluations

- Super-resolving downsampled images from 1.5-km to 750-m spatial resolution, and the original 750-m spatial resolution data are treated as ground truth.

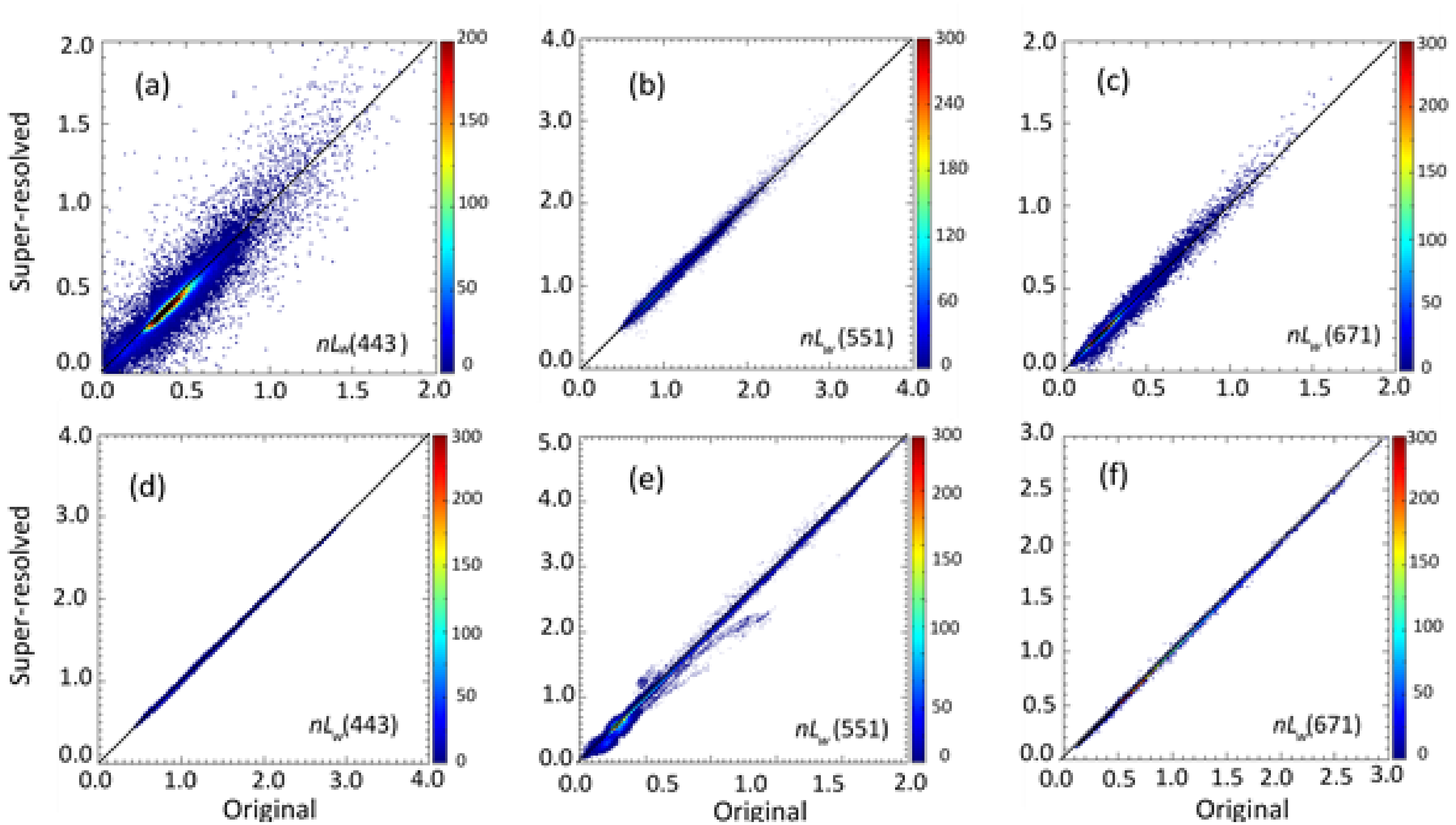

Density-scatter plot of super-resolved vs. original $nL_w(\lambda)$ images in Baltic Sea: Aug. 14, 2015 (top row); Bohai Sea: April 15, 2019 (bottom row)

Evaluations

Mean, **median**, and standard deviation (**STD**) of the ratio (super-resolved/original) and difference (diff) (super-resolved – original) between the super-resolved and original $nL_w(\lambda)$ images

	CNN-Baltic (ratio)			CNN-Bohai (ratio)			CNN-Baltic (diff)			CNN-Bohai (diff)		
	Mean	**Median**	**STD**	**Mean**	**Median**	**STD**	**Mean**	**Median**	**STD**	**Mean**	**Median**	**STD**
$nL_w(410)$	0.997	0.994	0.117	1.001	0.999	0.039	0.000	-0.001	0.078	-0.001	-0.001	0.027
$nL_w(443)$	0.997	0.996	0.099	1.000	1.000	0.021	-0.001	-0.001	0.075	-0.001	-0.001	0.022
$nL_w(486)$	1.000	0.999	0.070	0.990	0.999	0.067	0.000	-0.001	0.071	-0.001	-0.001	0.019
$nL_w(551)$	1.000	1.000	0.041	1.000	1.000	0.008	0.000	0.000	0.055	-0.001	-0.001	0.014
$nL_w(671)$	0.996	0.997	0.066	1.000	1.000	0.017	-0.001	-0.001	0.032	-0.001	0.000	0.015

Application to Original Scale

Baltic Sea: V2015226105214, acquired on August 14, 2015

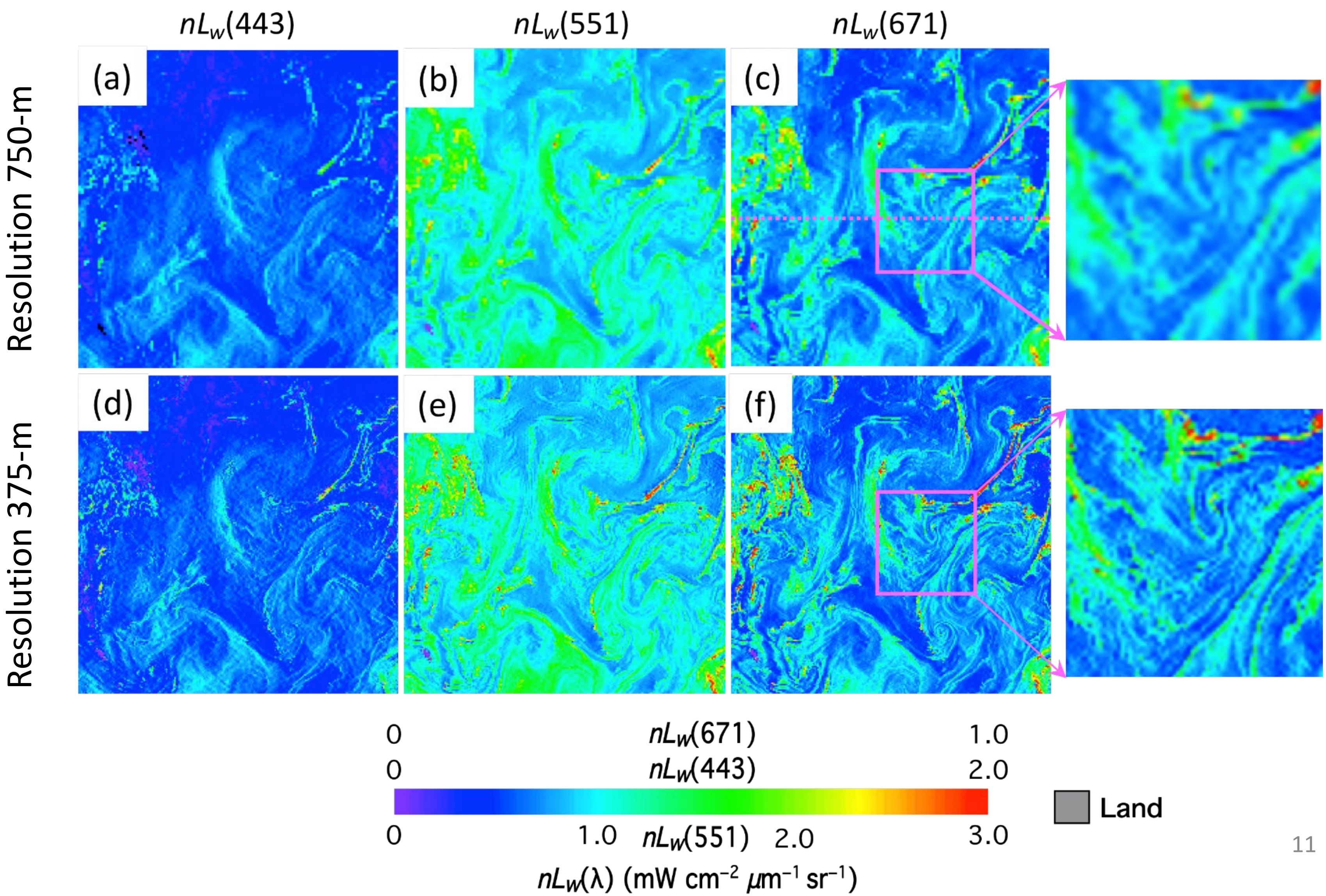

Application to Original Scale

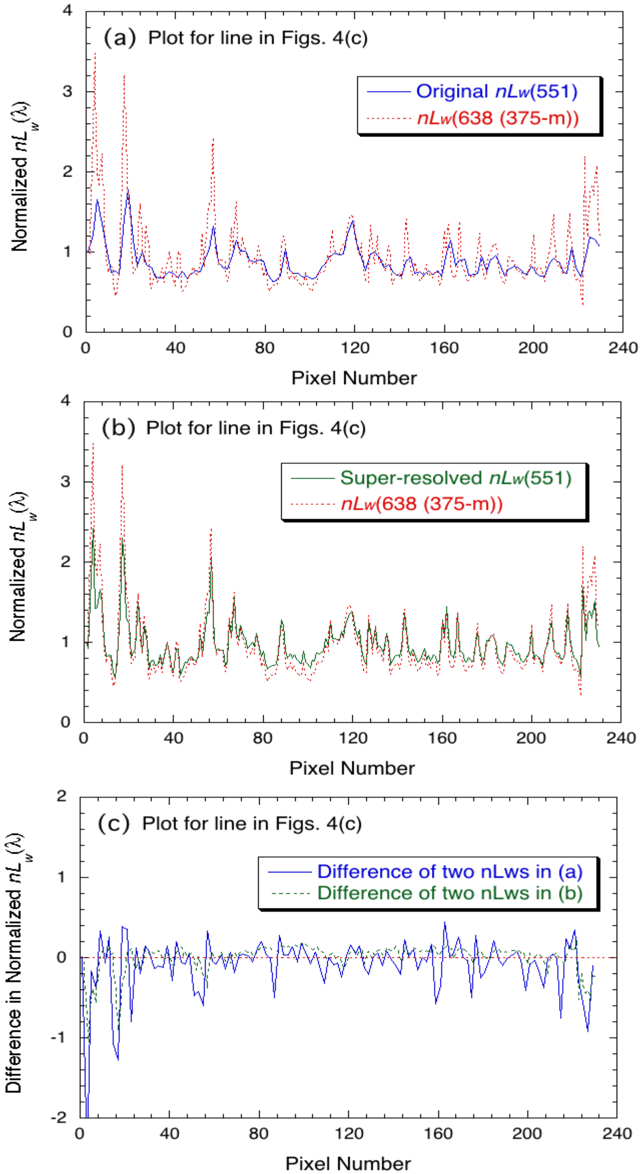

VIIRS-derived nLw(λ) along the pink dotted line in the last slide for (a) normalized original nLw(551) in blue solid line compared with those of nLw(638) in red, (b) normalized super-resolved nLw(551) in green solid line compared with those of nLw(638) in red, and (c) the difference between normalized original nLw(551) and nLw(638) (blue solid line), and between normalized super-resolved nLw(551) and nLw(638) (green dotted line).

Standard deviation (STD) of the difference between the original and super-resolved $nL_w(\lambda)$ image (normalized) with the $nL_w(638)$ along the pink line in last slide for the Baltic Sea and the pink line in the next slide for the Bohai Sea.

	STD (Baltic Sea)		**STD (Bohai Sea)**	
	Original – $nL_w(638)$	**Super-resolved – $nL_w(638)$**	**Original – $nL_w(638)$**	**Super-resolved – $nL_w(638)$**
$nL_w(410)$	0.4561	0.4182	0.1334	0.1291
$nL_w(443)$	0.4465	0.3551	0.1276	0.1235
$nL_w(486)$	0.3892	0.2633	0.1391	0.1358
$nL_w(551)$	0.3515	0.1773	0.1326	0.1264
$nL_w(671)$	0.3662	0.2393	0.0438	0.0433
$nL_w(745)$	0.2101	0.1125	0.1181	0.1024

Application to Original Scale

Bohai Sea: V2018252050036, acquired on Sep. 9, 2018

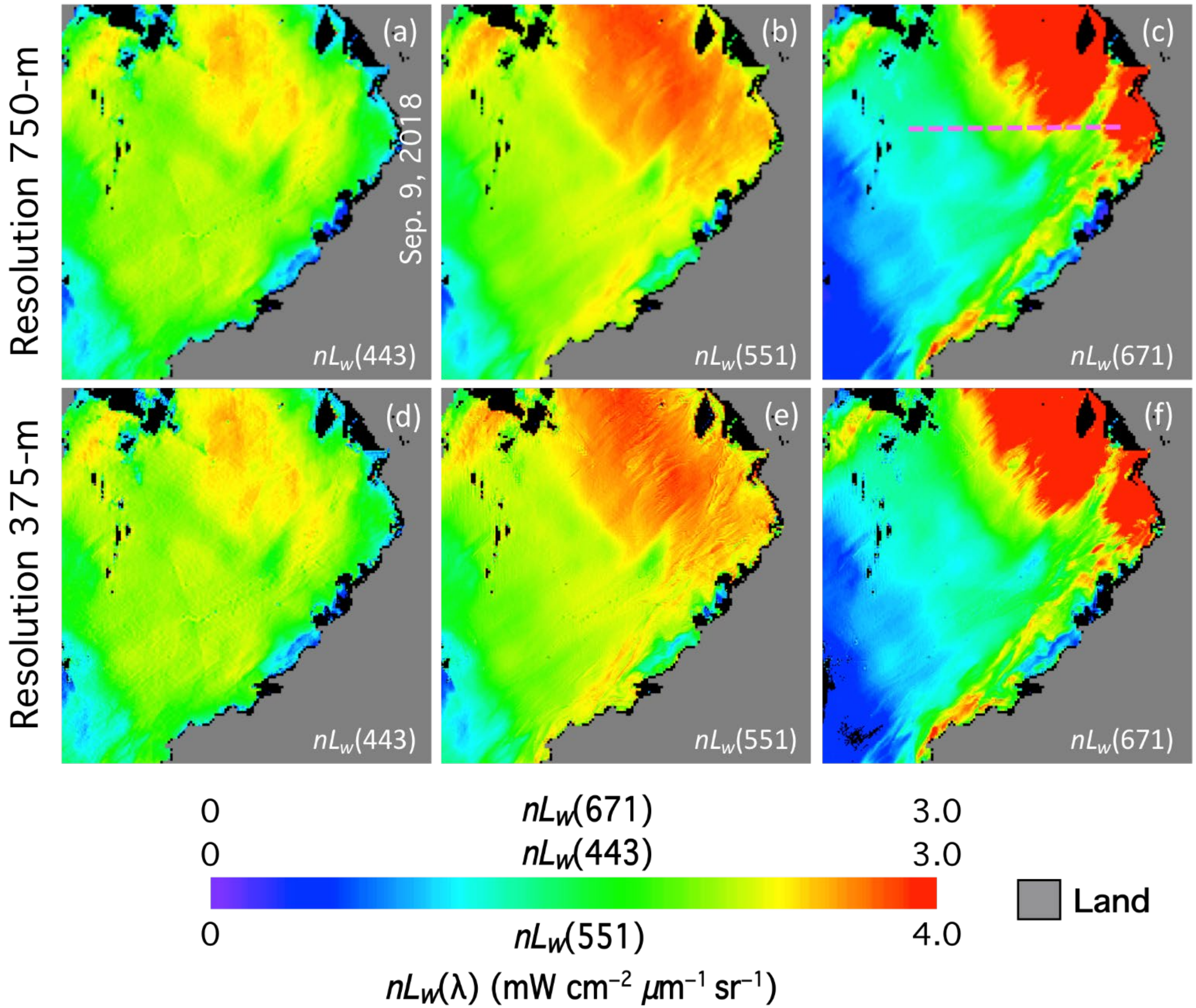

Applications

Chesapeake Bay (3 March 2018)

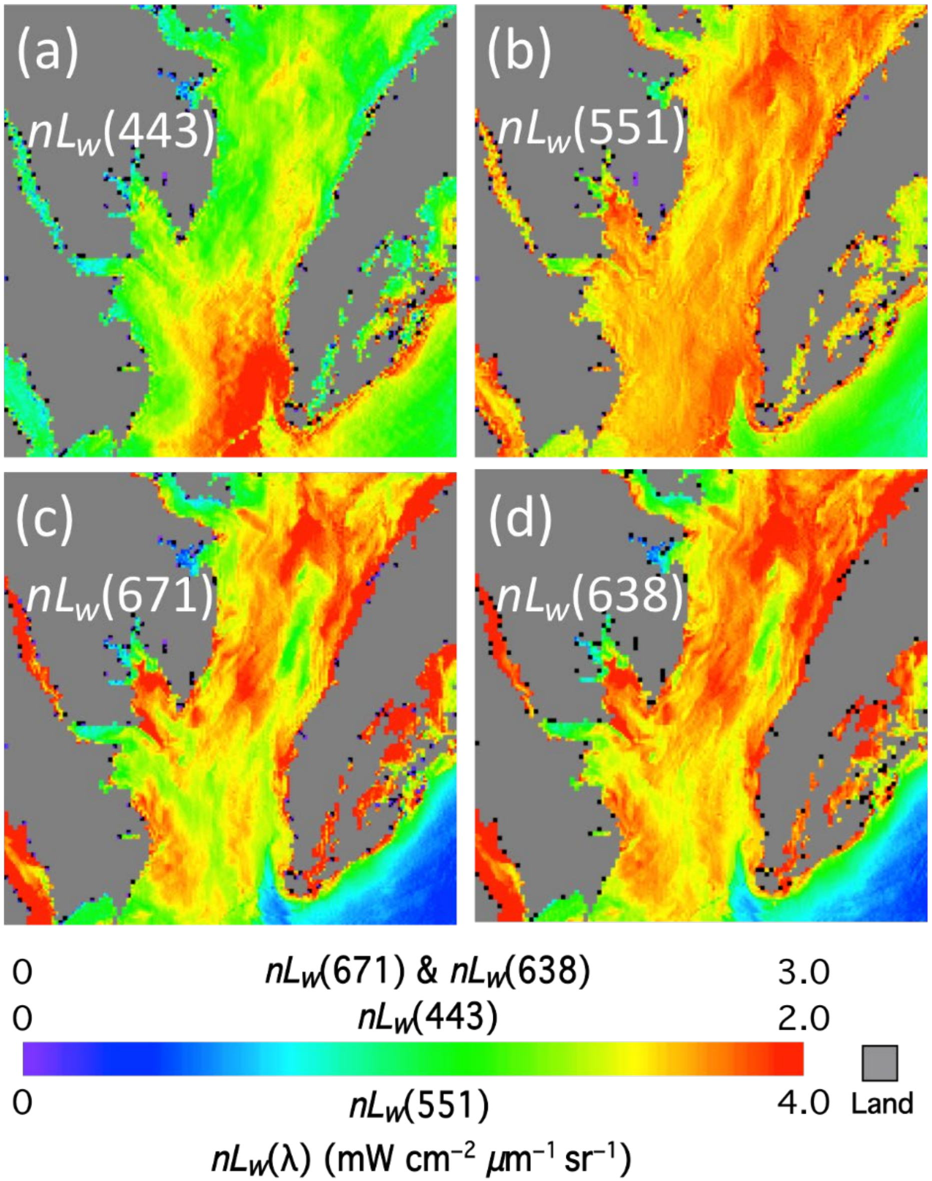

Gulf of Mexico (19 November 2019)

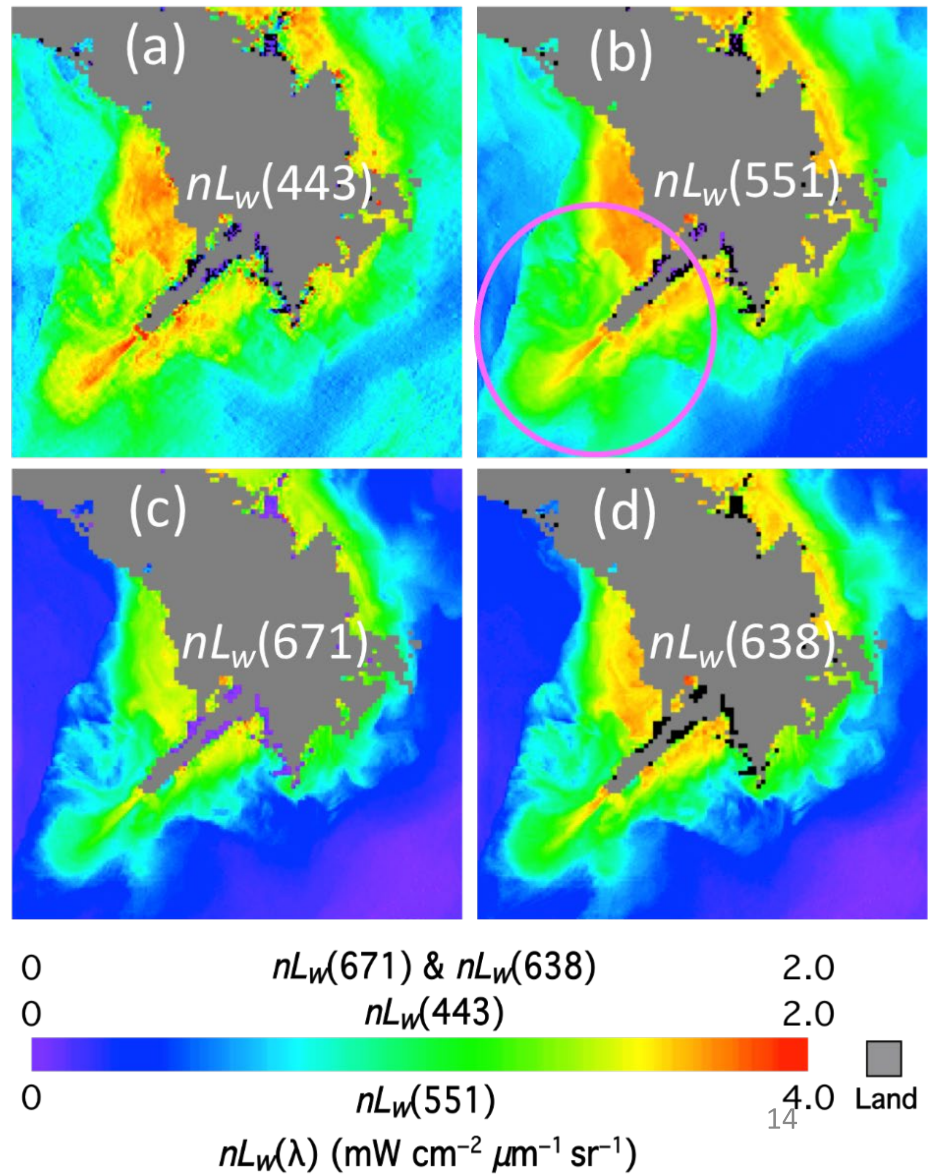

Applications

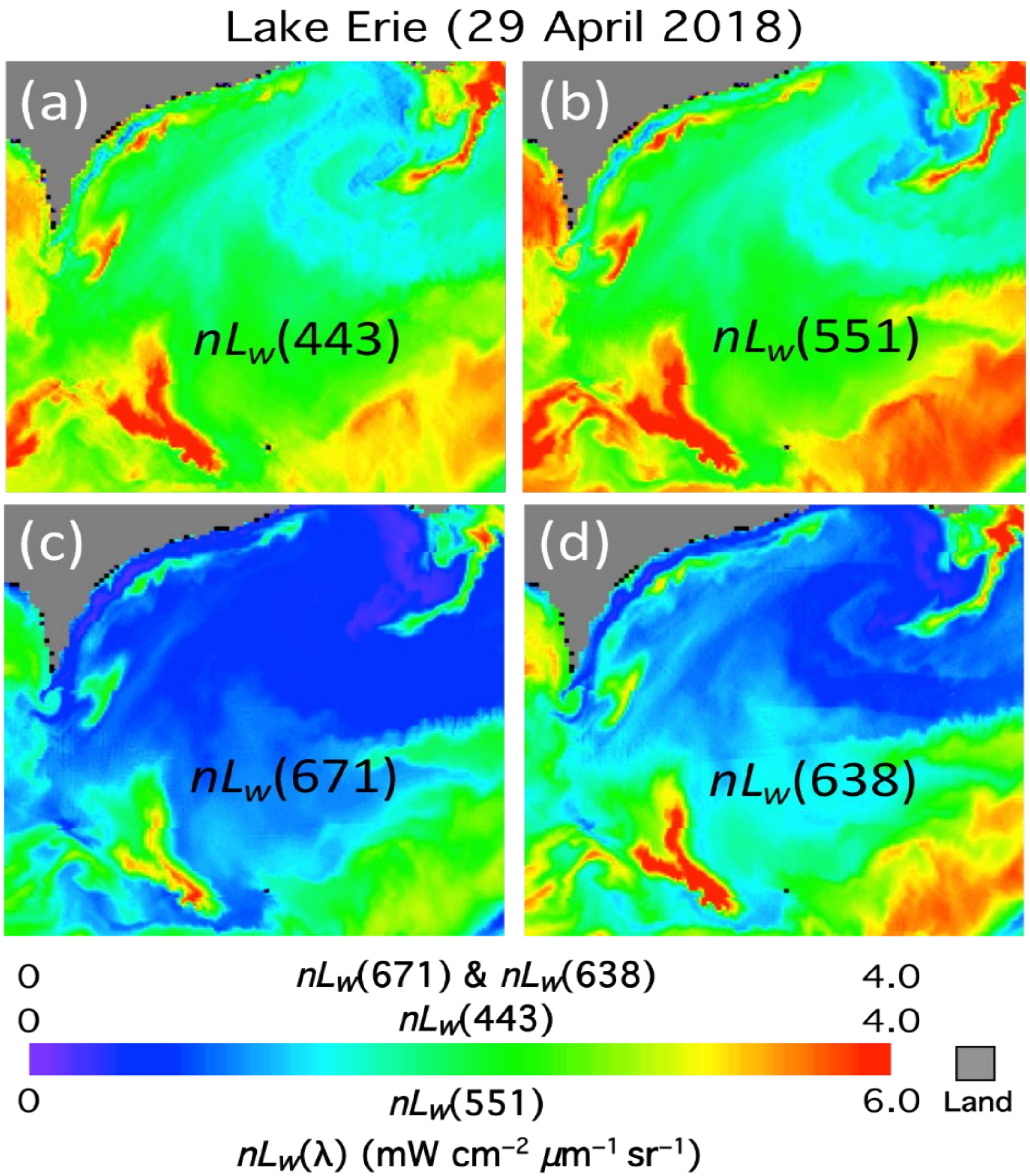

Applications

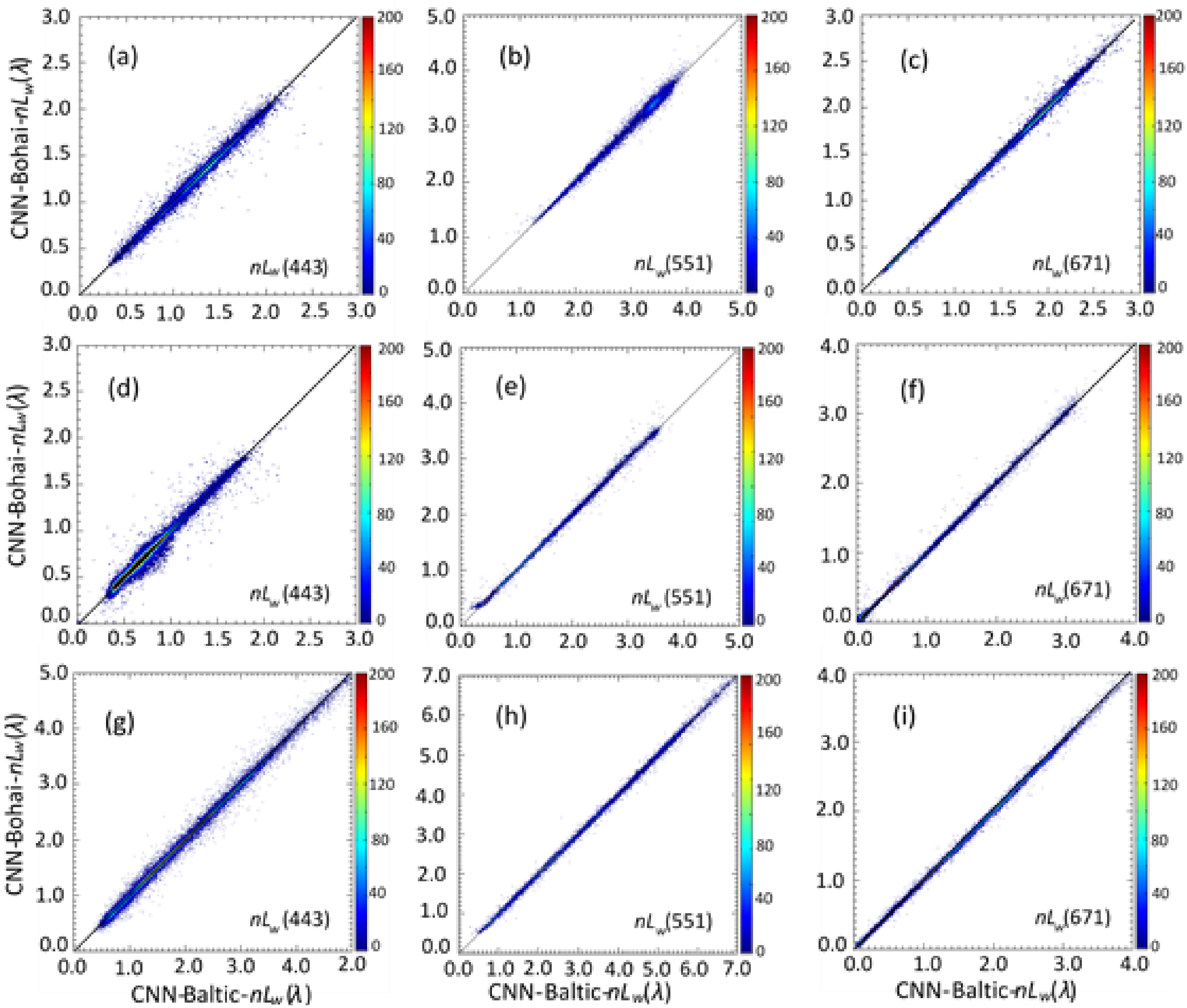

Density-scatter plot of super-resolved *$nL_w(\lambda)$* image derived from the Bohai model vs. Baltic model in Chesapeake Bay (top row), Gulf of Mexico (middle row), and Lake Erie (bottom row).

Applications

The **mean**, **median**, and **STD** of the $nL_w(\lambda)$ ratio between using the CNN-Bohai-$nL_w(\lambda)$ and CNN-Baltic-$nL_w(\lambda)$ in the Chesapeake Bay, Gulf of Mexico, and Lake Erie.

	Chesapeake Bay			Gulf of Mexico			Lake Erie		
	Mean	**Median**	**STD**	**Mean**	**Median**	**STD**	**Mean**	**Median**	**STD**
$nL_w(410)$	1.005	1.006	0.078	0.999	0.998	0.062	1.000	1.001	0.041
$nL_w(443)$	1.000	1.000	0.038	1.006	1.001	0.054	1.005	1.002	0.036
$nL_w(486)$	0.995	0.995	0.022	1.000	0.999	0.031	1.002	1.001	0.022
$nL_w(551)$	1.001	1.000	0.020	1.001	1.000	0.020	1.000	1.000	0.015
$nL_w(671)$	1.001	1.001	0.016	1.003	1.001	0.033	1.000	1.000	0.032

Part II: Super-resolving $K_d(490)$ and Chl-a

Super-resolving $K_d(490)$ and Chl-a

- We do not directly super-resolve $K_d(490)$ and Chl-a images from coarse resolution to fine resolution. Rather, high-resolution $K_d(490)$ and Chl-a images are derived from super-resolved $nL_w(\lambda)$ images.
- The $K_d(490)$ algorithm is a combination of standard (for clear oceans) and turbid $K_d(490)$ models for accurate retrieval of $K_d(490)$ products for both clear and turbid ocean waters.
  - M. Wang, S. Son, and J. L. W. Harding, "Retrieval of diffuse attenuation coefficient in the Chesapeake Bay and turbid ocean regions for satellite ocean color applications," *J. Geophys. Res.*, vol. 114, C10011, http://dx.doi.org/10.1029/2009JC005286, 2009.
- The Chl-a algorithm uses the ocean color index (OCI) method, which has been proved to be more stable than the classic OCx-based algorithm.
  - M. Wang and S. Son, "VIIRS-derived chlorophyll-a using the ocean color index method," *Remote Sens. Environ.*, vol. 182, pp. 141–149, 2016.

Training Dataset

	Baltic Sea		Bohai Sea		La Plata Estuary	
Case	**Granule**	**Date**	**Granule**	**Date**	**Granule**	**Date**
1	V2019070042852	03/11/2019	V2015213113614	08/01/2015	V2020019175116	01/19/2020
2	V2019073051140	03/14/2019	V2015215105822	08/03/2015	V2020046174522	02/15/2020
3	V2019073051305	03/14/2019	V2015216103927	08/04/2015	V2020057173912	02/26/2020
4	V2019074045411	03/15/2019	V2015221104550	08/09/2015	V2020062174536	03/02/2020
5	V2019075043516	03/16/2019	V2015223114859	08/11/2015	V2020063172640	03/03/2020
6	V2019084050531	03/25/2019	V2015225111108	08/13/2015	V2020073173926	03/13/2020
7	V2019090045259	03/31/2019	V2015227103444	08/15/2015	V2020083175048	03/23/2020
8	V2019091043404	04/01/2019	V2015228115523	08/16/2015	V2020084173317	03/24/2020
9	V2019100050545	04/10/2019	V2015229113502	08/17/2015	V2020095172707	04/04/2020
10	V2019106045313	04/16/2019	V2015229113627	08/17/2015	V2020109180347	04/18/2020
11	V2019116050558	04/26/2019	V2015230111606	08/18/2015	V2020110174451	04/19/2020
12	V2019121051222	05/01/2019	V2015230111731	08/18/2015	V2020111172557	04/20/2020
13	V2019126051846	05/06/2019	V2015231105836	08/19/2015	V2020131175128	05/10/2020
14	V2019127045950	05/07/2019	V2015232103942	08/20/2015	V2020133171337	05/12/2020
15	V2019143050004	05/23/2019	V2015235112355	08/23/2015	V2020137173857	05/16/2020

https://www.star.nesdis.noaa.gov/sod/mecb/color/

Re-Training Networks

La Plata River Estuary, February 27, 2020

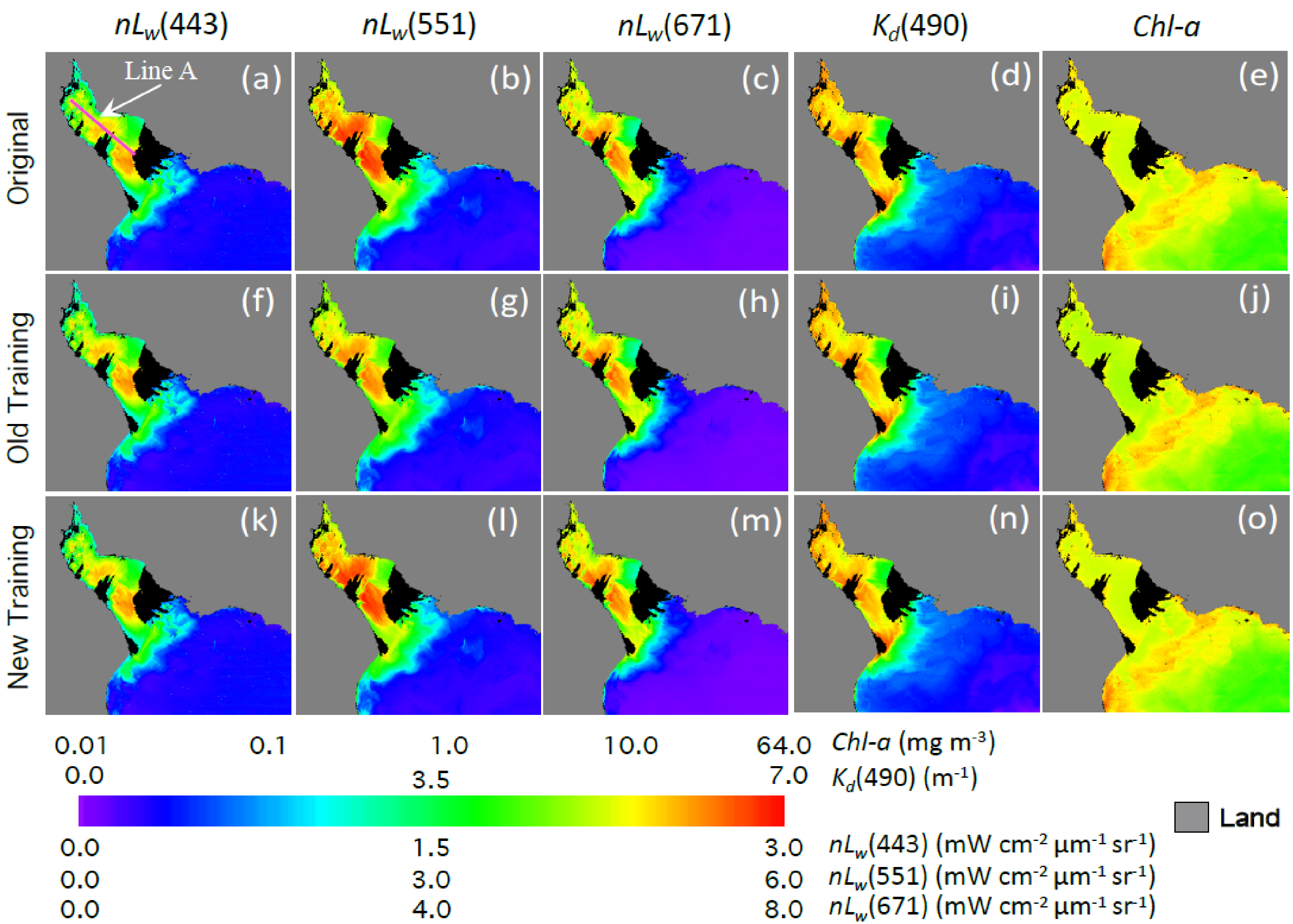

Re-Training Networks

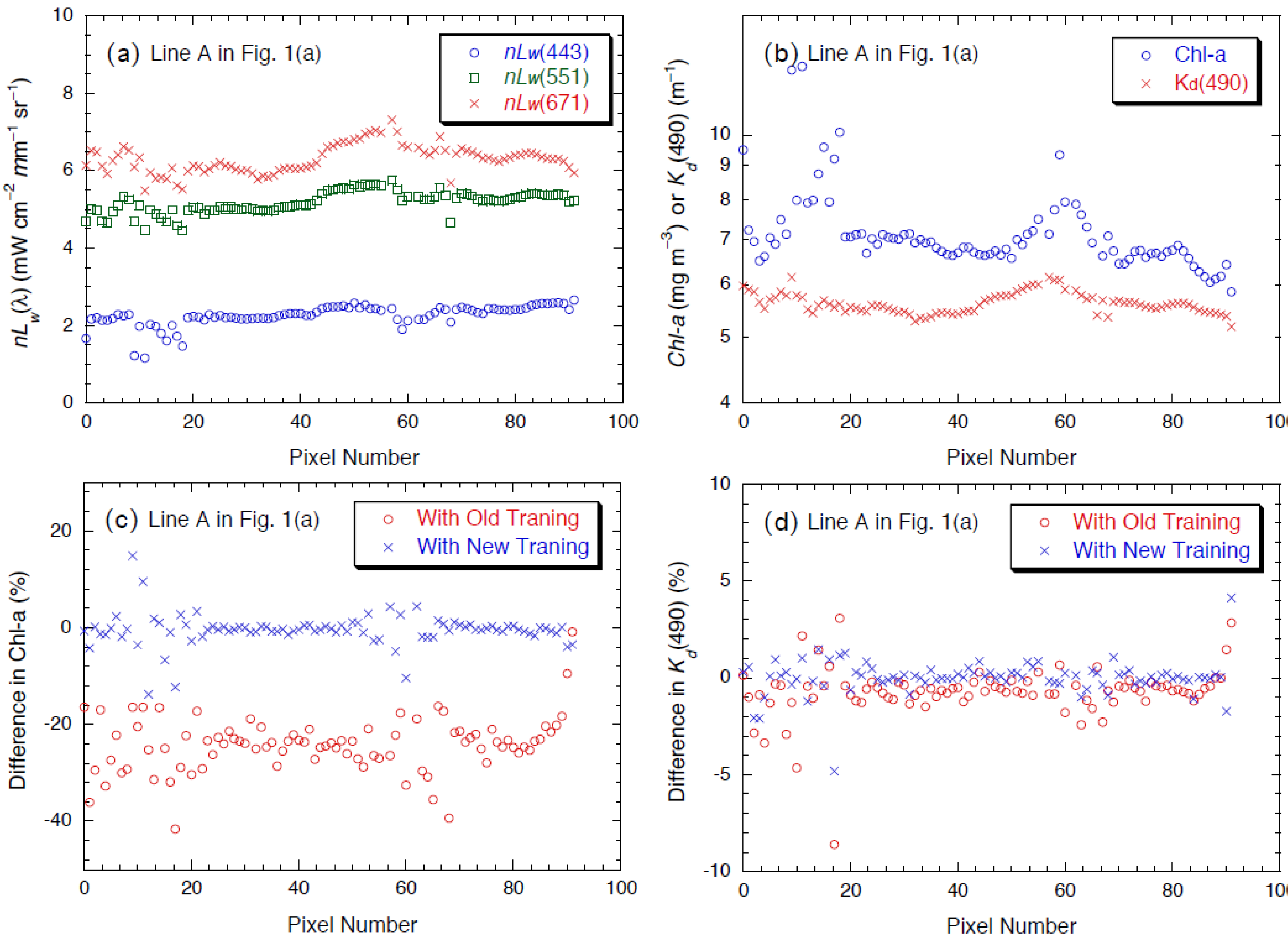

Evaluations (1)

Baltic Sea: V2015226105214, acquired on August 14, 2015

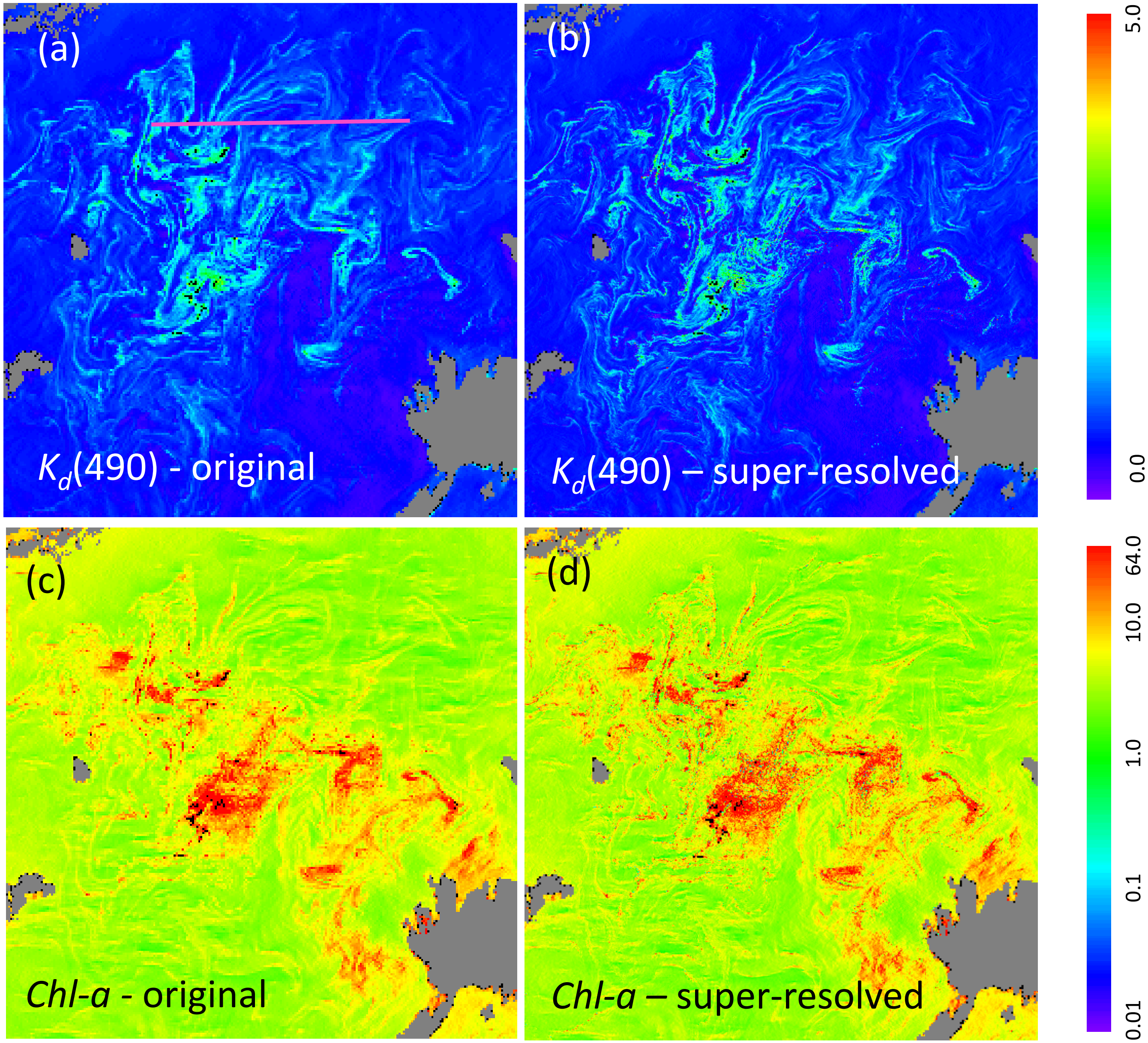

Evaluations (2)

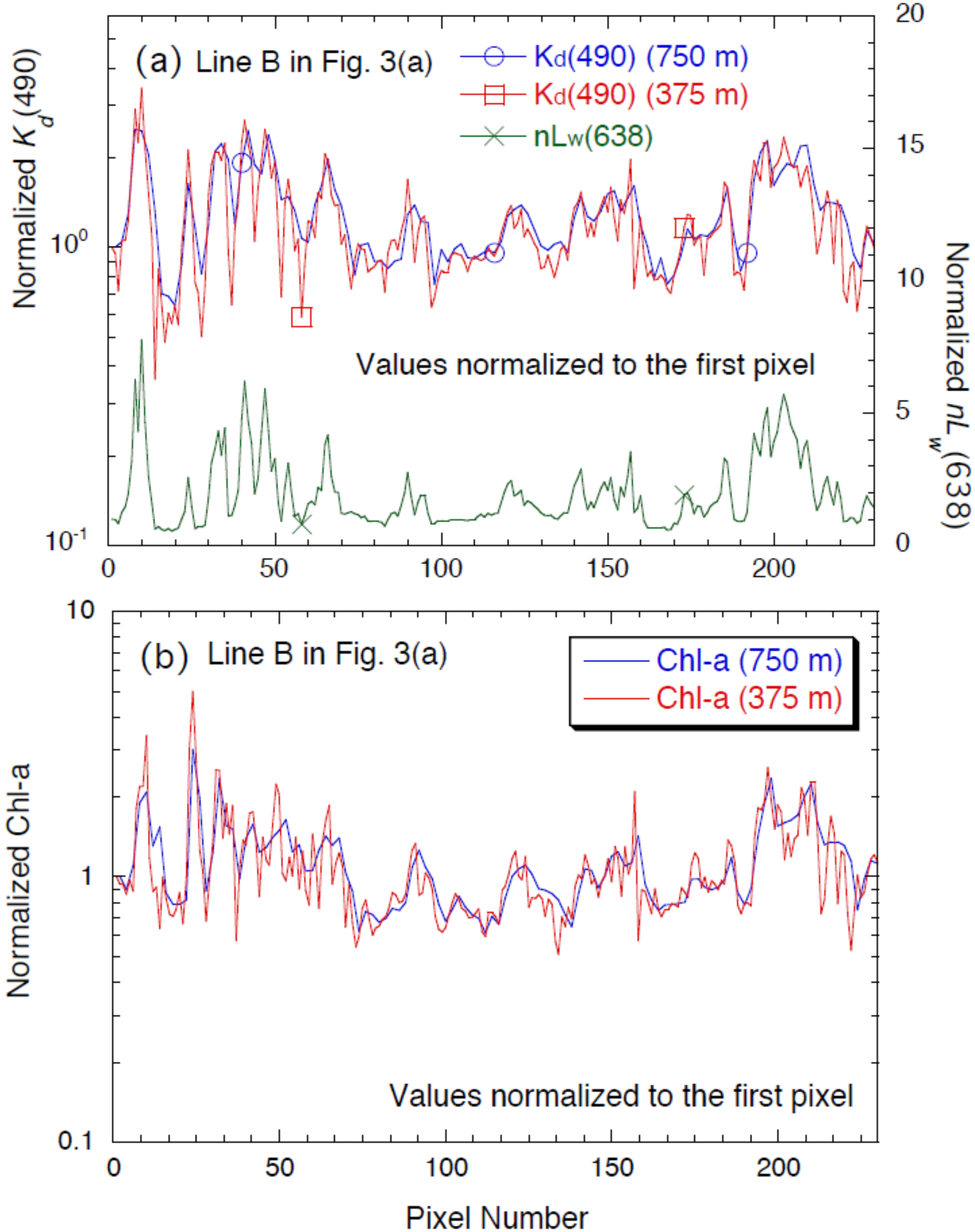

Evaluations (3)

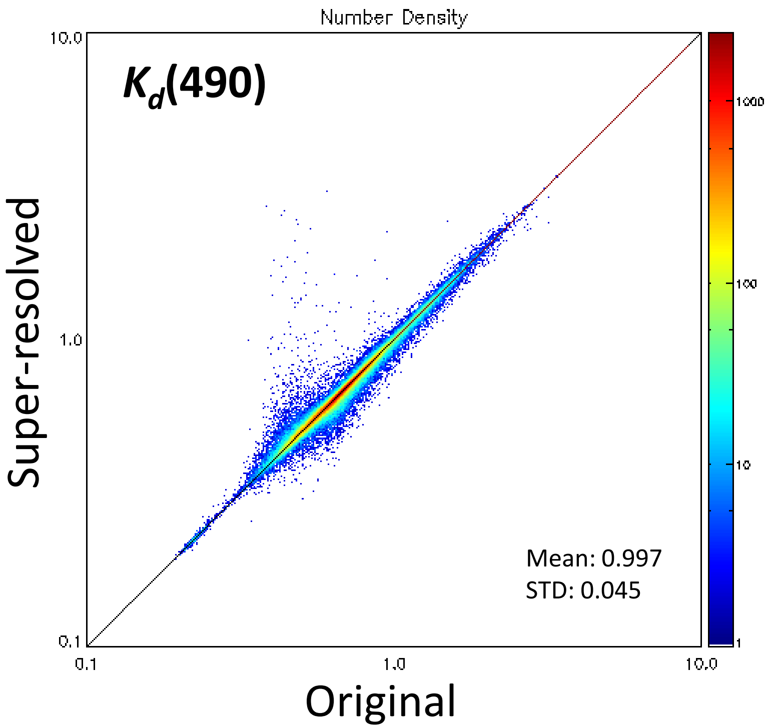

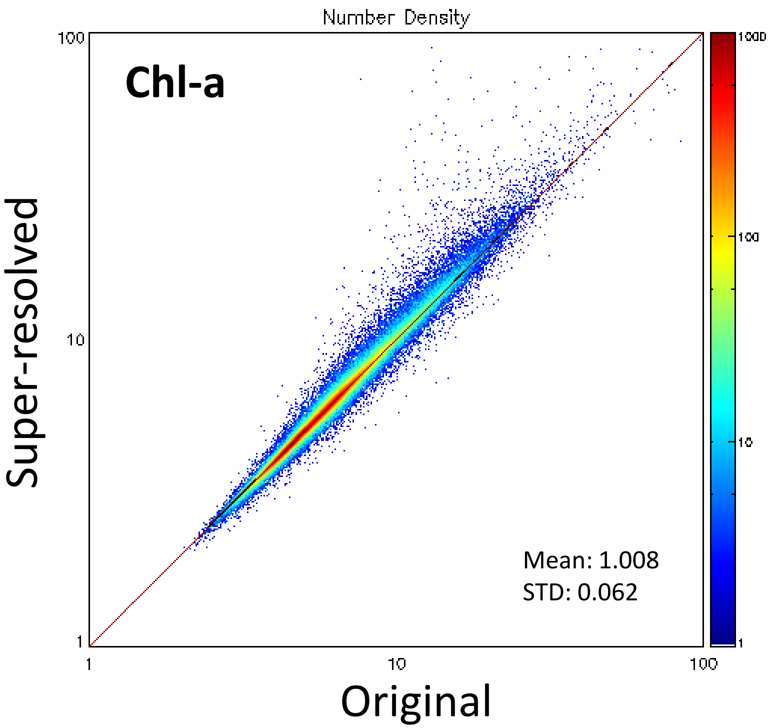

Application to Lake Erie

Lake Erie on April 29, 2018 (V2018119182603)

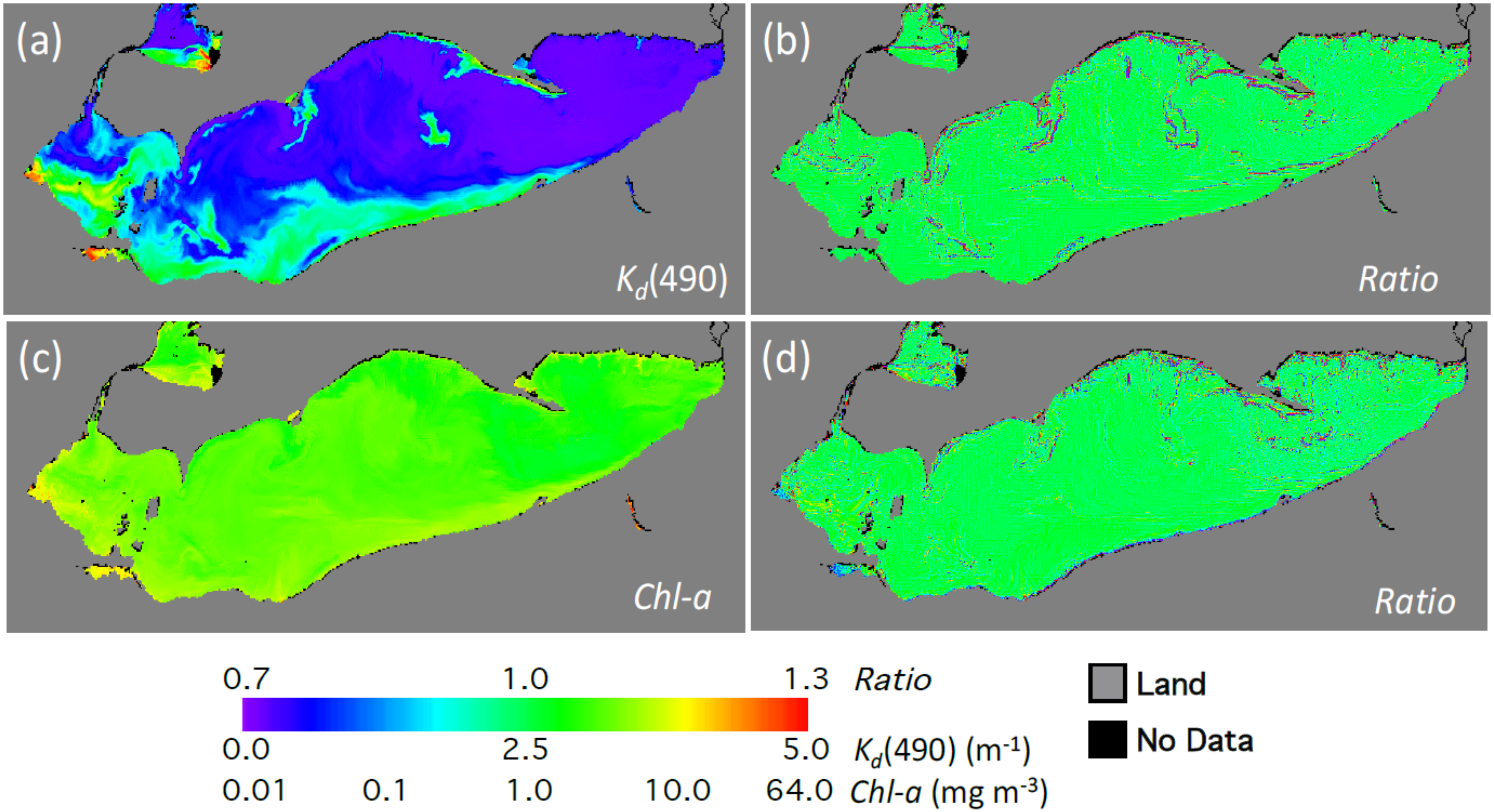

Application to the Bohai Sea

Bohai Sea, September 9, 2018 (Granule V2018252050036)

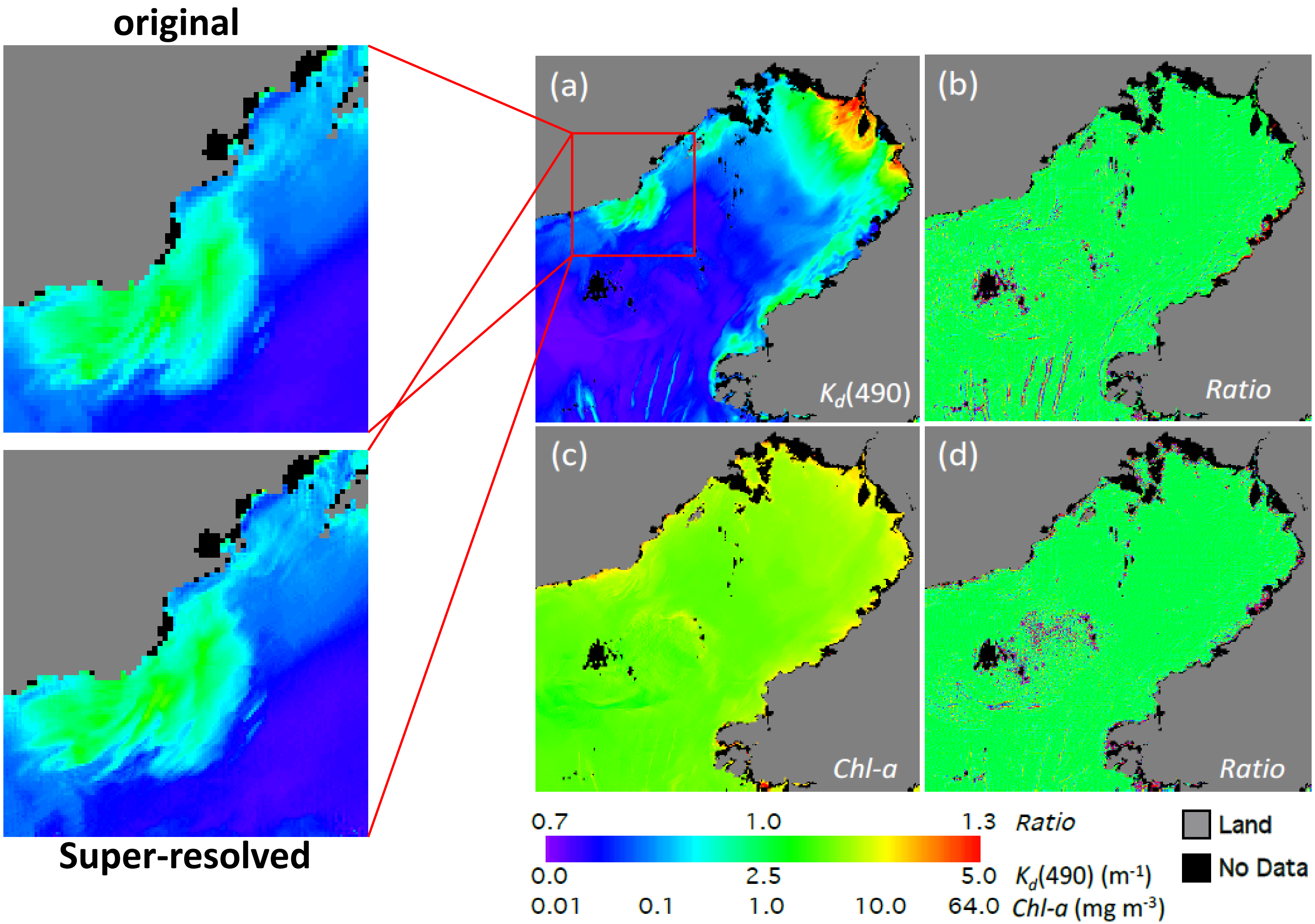

Application to the Gulf of Mexico

Gulf of Mexico, November 19, 2019 (V2019323185429)

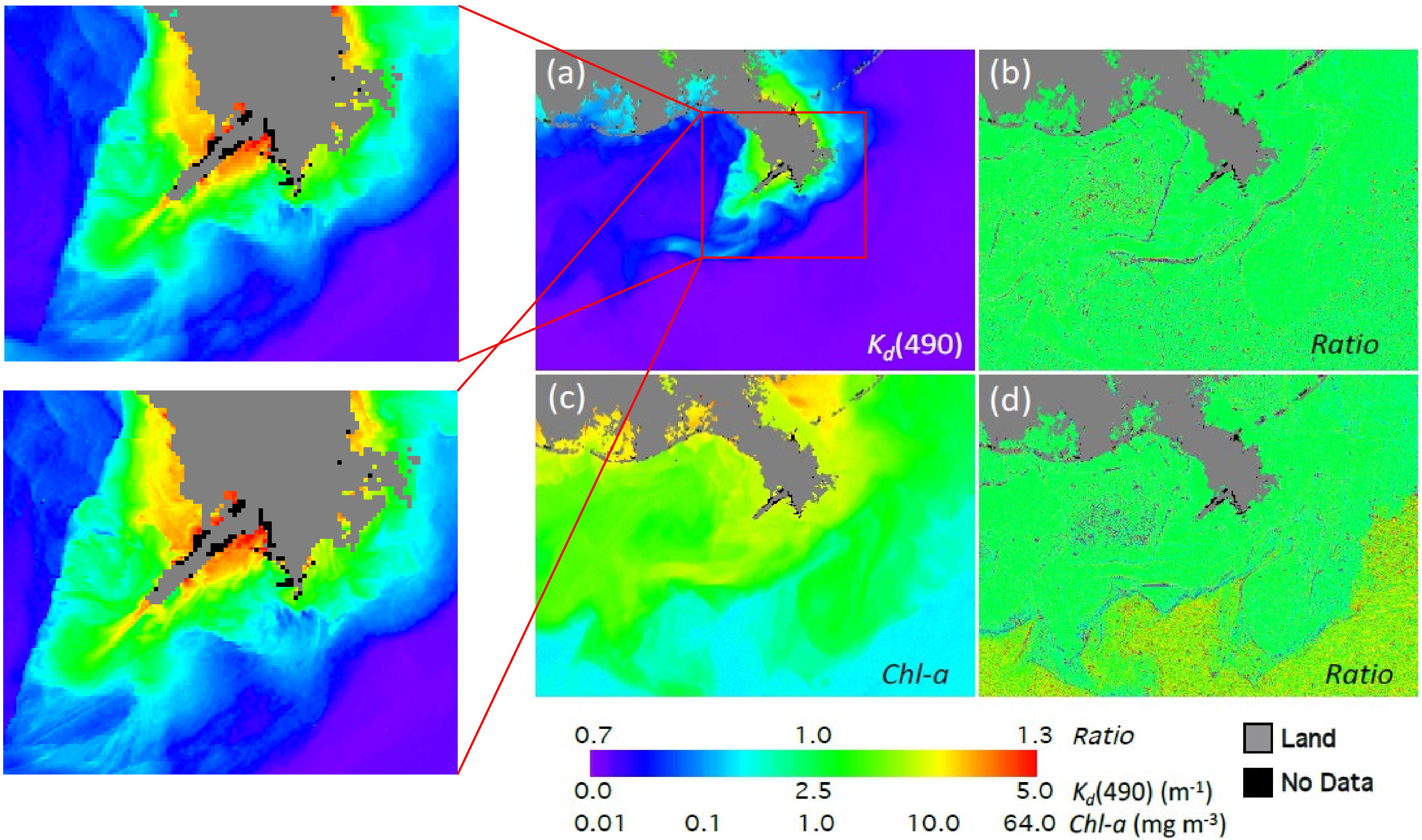

Application to the Chesapeake Bay

Chesapeake Bay, March 3, 2018 (V2018062175339)

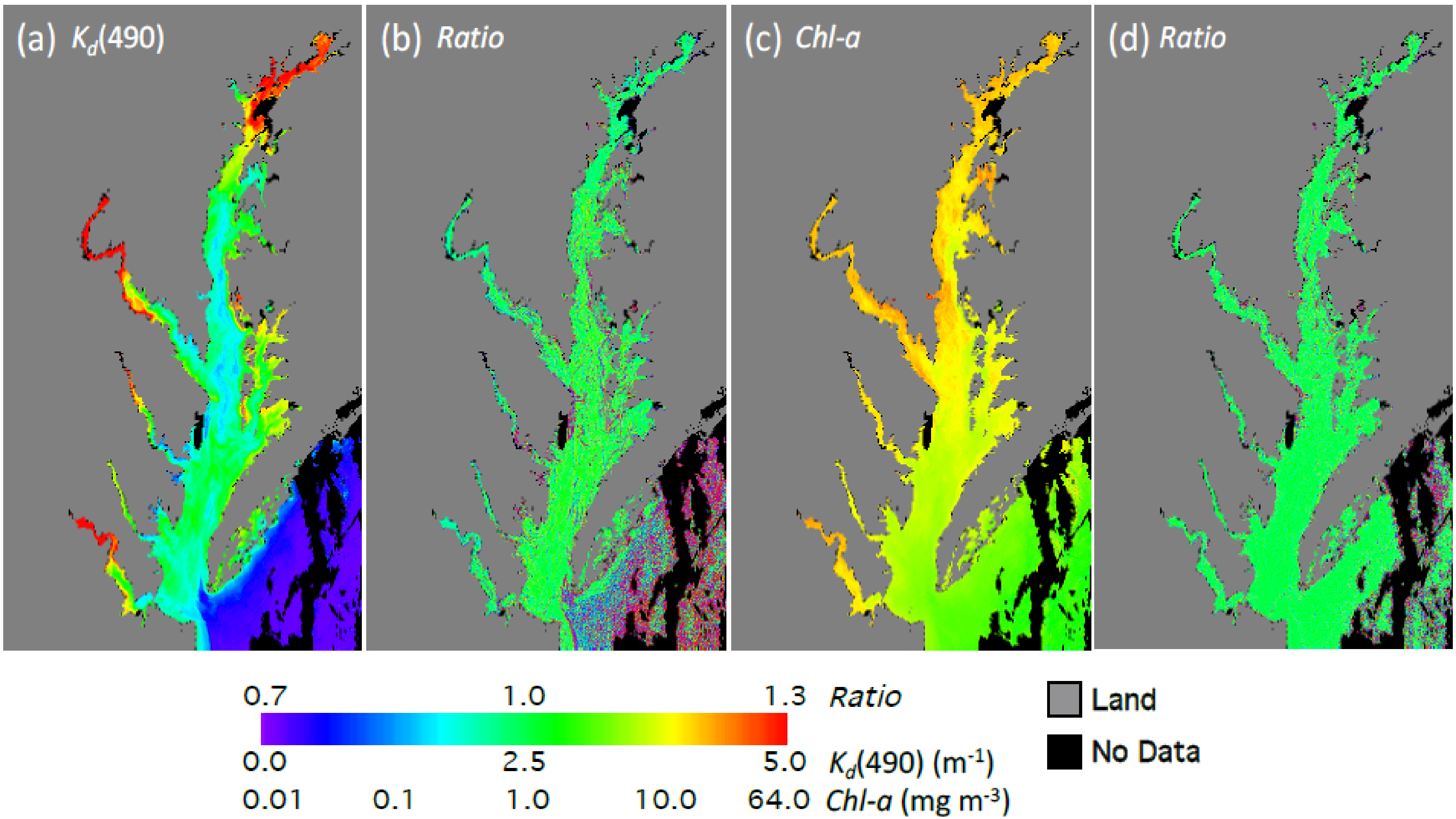

Statistics Results

The **mean**, **median**, and **STD** of the super-resolved/original ratio of $K_d(490)$ and Chl-a in the Bohai Sea, Chesapeake Bay, Lake Erie and Gulf of Mexico.

	Bohai Sea			Chesapeake Bay			Lake Erie			Gulf of Mexico		
	Mean	Median	STD	Mean	Median	STD	Mean	Median	STD	Mean	Median	STD
$K_d(490)$	1.003	1.000	0.056	1.010	1.000	0.111	0.998	1.000	0.076	1.002	1.000	0.066
Chl-a	0.999	1.000	0.060	1.004	1.000	0.094	0.995	0.997	0.080	1.015	1.000	0.128

Summary and Path Forward

- Deep convolutional neural network (**CNN**) is used to super-resolve VIIRS M-band $nL_w(\lambda)$ from 750-m to 375-m spatial resolution.
- High-resolution (375-m) super-resolved $nL_w(\lambda)$ images are much sharper, and show more fine structures than the original $nL_w(\lambda)$ images. Therefore, practically the performance of the networks is acceptable for super-resolving $nL_w(\lambda)$ images of the all VIIRS six M-bands to 375-m spatial resolution.
- High spatial resolution Chl-a and $K_d(490)$ are further derived from $nL_w(\lambda)$.
- We are working on the implementation of the networks for routine VIIRS ocean color data processing to super-resolve VIIRS M-band $nL_w(\lambda)$ images in coastal and inland waters.
- Applications to other satellite sensors, such as **VIIRS** on the NOAA-20, the Operational Land Imager (**OLI**) on the Landsat-8 and the Ocean and Land Colour Instrument (**OLCI**) on the Sentinel-3A/3B, will be tested.